JCB Report

Secretory vesicle transport velocity in living cells depends on the myosin-V lever arm length

Daniel H. Schott,[1] Ruth N. Collins,[2] and Anthony Bretscher[1]

[1]Department of Molecular Biology and Genetics and [2]Department of Molecular Medicine, Cornell University, Ithaca, NY 14853

Myosins are molecular motors that exert force against actin filaments. One widely conserved myosin class, the myosin-Vs, recruits organelles to polarized sites in animal and fungal cells. However, it has been unclear whether myosin-Vs actively transport organelles, and whether the recently challenged lever arm model developed for muscle myosin applies to myosin-Vs. Here we demonstrate in living, intact yeast that secretory vesicles move rapidly toward their site of exocytosis. The maximal speed varies linearly over a wide range of lever arm lengths genetically engineered into the myosin-V heavy chain encoded by the *MYO2* gene. Thus, secretory vesicle polarization is achieved through active transport by a myosin-V, and the motor mechanism is consistent with the lever arm model.

Introduction

Organelle movement has intrigued scientists ever since cytoplasmic streaming was first seen by Corti (1774). Type-V myosins are probably specialized as organelle motors, as myosin-Vs are needed for the correct distribution of a wide variety of membranes within animal and fungal cells (Reck-Peterson et al., 2000), whereas the closely related myosin-XIs may drive membrane streaming in plant cells (Kashiyama et al., 2000). However, in at least some animal cells, myosin-V appears to determine the organelle distribution by passively tethering organelles that reach the cell periphery (Wu et al., 1999). Direct demonstration that a myosin-V/XI actively transports membranes in intact cells has remained elusive.

Active transport of membranes by myosin-V has been questioned in fungal cells as well. The budding yeast *Saccharomyces cerevisiae* tightly concentrates post-Golgi secretory vesicles to polarized sites at the cell surface, a process that requires the myosin-V heavy chain Myo2p (Johnston et al., 1991; Govindan et al., 1995; Schott et al., 1999) and polarized cables of actin filaments (Pruyne et al., 1998). Because nearly all of the Myo2p is at these sites, and at least some can concentrate there independently of actin (Ayscough et al., 1997), Myo2p has been proposed to target vesicles by passive capture (Reck-Peterson et al., 2000).

We investigated this by following the itinerary of secretory vesicles in live cells. The ease with which we could genetically modify Myo2p's motor properties not only allowed us to determine whether Myo2p is the motor for vesicle movement, but also allowed us to test models of how myosin produces force. The swinging lever arm model predicts that the light chain binding region of the myosin heavy chain forms a rigid rod, or lever arm, that amplifies small movements of the actin-binding globular domain (Uyeda et al., 1996; Geeves and Holmes, 1999; Houdusse and Sweeney, 2001; Fig. 1). If so, the step size and therefore the sliding velocity are predicted to be proportional to the length of this rod. Although this model has recently been disputed (Yanagida et al., 2000b; Yanagida and Iwane, 2000), studies of purified myosin-II, which normally has a short predicted lever arm of two light chain binding (IQ) repeats, have shown that velocity and step size are proportional to the predicted lever arm length up to one and a half times the natural length (Uyeda et al., 1996; Ruff et al., 2001). In contrast, an experiment on myosin-V, which normally has six IQ repeats (Fig. 1 A), showed a similar velocity for a 2-IQ version as for wild-type version (Trybus et al., 1999). Such in vitro studies are complicated by interactions between the myosin and the surface it is attached to, and by the difficulty of duplicating the physiological orientation of the myosin molecule (Yanagida et al., 2000a). Therefore, an in vivo assay would be an important tool.

Address correspondence to Anthony Bretscher, Dept. of Molecular Biology and Genetics, 351 Biotechnology Bldg., Cornell University, Ithaca, NY 14853. Tel.: (607) 255-5713. Fax: (607) 255-2428. E-mail: apb5@cornell.edu

Key words: exocytosis; *Saccharomyces*; molecular motors; myosin; cell polarity

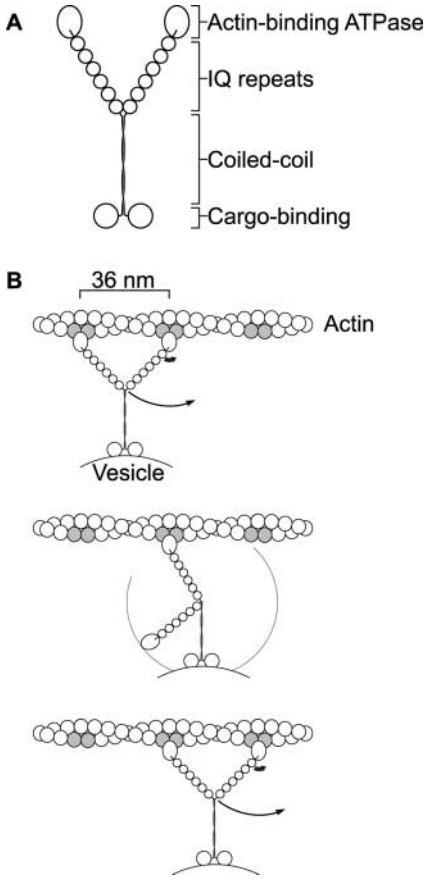

Figure 1. **Structure and model of myosin-V.** (A) Schematic diagram of myosin-V (Cheney et al., 1993). NH_2-terminal actin-binding ATPase domain sequences, the six IQ repeats, the coiled-coil region, and COOH-terminal globular domain sequences are conserved in animals, fungi, plants, and slime mold. (B) Swinging lever arm model proposed for the walking of a myosin-V dimer along actin (Rief et al., 2000; Mehta, 2001). Conformational changes in the actin-binding domain during its ATPase cycle (thick arrow) rotates the lever arm, resulting in movement (thin arrow). The repeated binding sites are highlighted in gray.

Results and discussion

Post-Golgi secretory vesicles show linear, polarized movement inside intact cells

To test whether vesicles actively move toward sites of exocytosis, we observed living cells producing green fluorescent protein (GFP)* fused with Sec4p, which resides specifically on the surface of secretory vesicles (Mulholland et al., 1997; Walch-Solimena et al., 1997; Fig. 2 A). The GFP–Sec4p fluorescence matches the Sec4p distribution reported for anti-Sec4p immunofluorescence and immunoelectron microscopy, namely concentrated at sites of exocytosis (Fig. 2 B). In cells with medium-sized buds, most of the GFP–Sec4p is seen in a churning mass at the bud tip, likely reflecting continual congregation of secretory vesicles there, while the mother cell contains only a few particles 30- to 200-fold dimmer than the bud tip. These particles are smaller than the microscope's resolution, and may be single vesicles or small clusters. Many of these particles move across the mother cell, with an average velocity of 3 μm/s (Figs. 2 C and 5; Video 1, available at http://www.jcb.org/cgi/content/full/jcb.200110086/DC1). 99% of these movements are toward the bud neck and often more than one particle follows the same linear track, suggestive of actin cables. We also see particles moving in a directed manner through the bud neck to the bud tip (Fig. 3 A; Video 2, available at http://www.jcb.org/cgi/content/full/jcb.200110086/DC1). We conclude that secretory vesicles reach their destination by active transport.

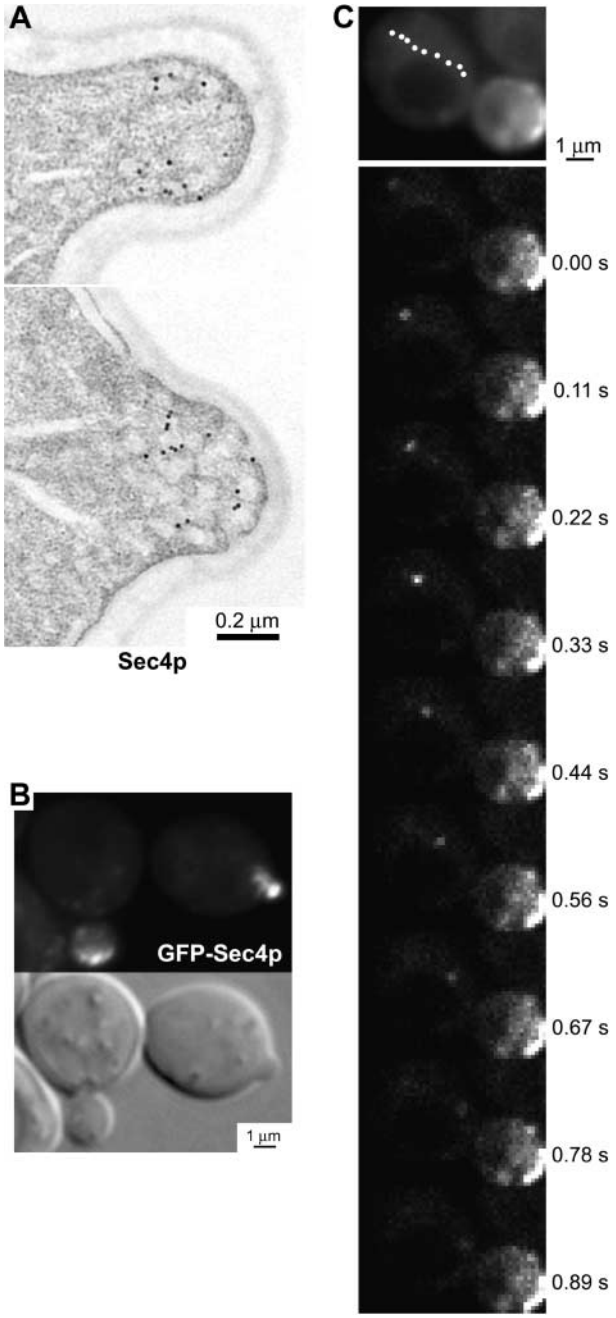

Figure 2. **Secretory vesicle movement.** (A) Secretory vesicles in small buds. 10-nm gold labels Sec4p in these immunoelectron micrographs, performed as described (Mulholland et al., 1997). (B) Fluorescence and Nomarski images of live cells containing GFP–Sec4p. (C) Linear movement of a GFP–Sec4p particle in a wild-type cell. The nine frames span 0.89 s. See Video 1, available at http://www.jcb.org/cgi/content/full/jcb.200110086/DC1.

*Abbreviation used in this paper: GFP, green fluorescent protein.

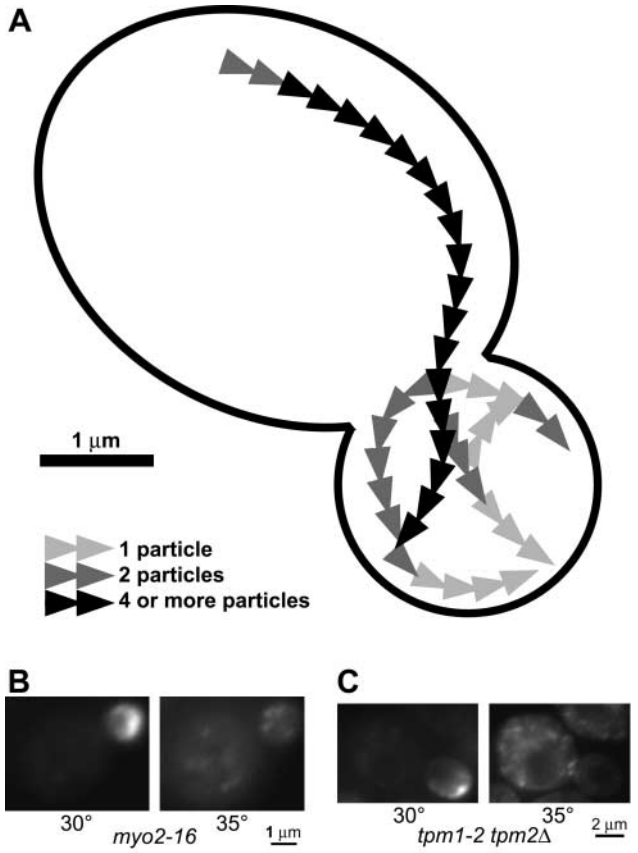

Figure 3. **Secretory vesicles follow defined tracks and their transport depends on actin cables and myosin.** (A) Paths taken by GFP–Sec4p particles in one wild-type cell over the course of 18 s. See Video 2, available at http://www.jcb.org/cgi/content/full/jcb.200110086/DC1. (B) GFP–Sec4p in a *myo2–16* cell at 30°C, and 7 min later at 35°C. (C) GFP–Sec4p in a *tpm1–2 tpm2Δ* cell at 30°C, and 5 min later at 35°C. See Video 3.

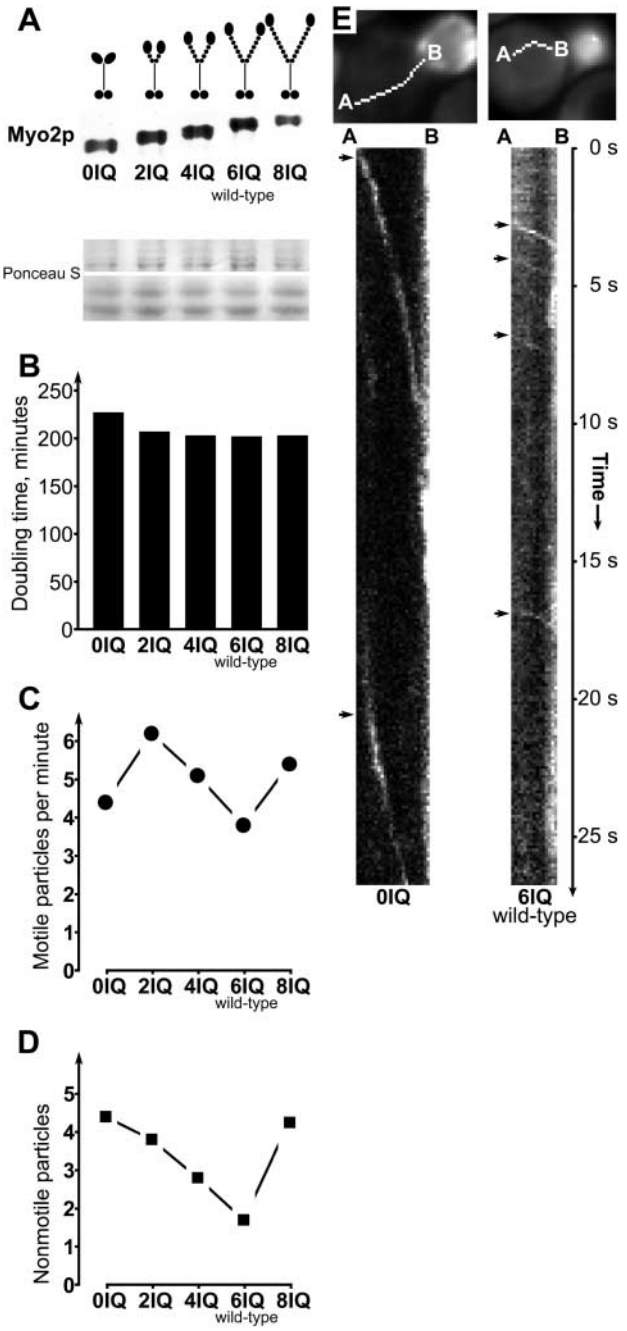

Figure 4. **Myo2p with zero, two, four, and eight IQ repeats is functional.** (A) Myo2p Western blot of strains used. Also shown is Ponceau S staining of major protein bands on the same blot (migrating at ~220 kD, upper box, and ~60 kD, lower box), as a loading control (see Materials and methods). (B) Doubling times of strains at 25°C in defined medium. (C) Frequency of particles showing linear movement in the mother cell in one plane. (D) Number of nonmotile particles in the mother cell in one plane. Since the motile particles transit rapidly across a cell, the majority of particles seen in the mother cell at any one moment are stationary. (E) Plots of fluorescence intensity along the lines shown at top from points A to B, versus time (kymograph) for a *MYO2–0IQ* cell (left) and a *MYO2* wild-type cell (6IQ, right).

The *myo2–16* mutant is conditionally defective for the association of secretory vesicles with Myo2p (Schott et al., 1999), and the *tpm1–2 tpm2Δ* mutant is conditionally defective for actin cables (Pruyne et al., 1998). Both mutants cease linear GFP–Sec4p movement upon shift to the restrictive temperature, and within minutes the mother cell contains many GFP–Sec4p particles showing Brownian motion (Fig. 3, B and C; Video 3, available at http://www.jcb.org/cgi/content/full/jcb.200110086/DC1). This suggests that the linear transit of vesicles across cells requires actin cables and myosin.

The number of IQ repeats in myosin-V determines secretory vesicle velocity

The active movement of vesicles in living, intact cells allows us to test models of the myosin motor mechanism in a truly physiological setting. As mentioned above, lever arm models predict that velocity should be proportional to the lever arm length under ideal conditions for motility. Therefore, we made a series of otherwise identical yeast strains containing zero, two, four, six, and eight IQ repeats in the sole copy of the *MYO2* gene (Fig. 4 A). Growth rates for these strains are identical to wild-type strains, except for the 0IQ variant that grows 10% slower, as reported by Stevens and Davis (1998). This indicates that all of the constructs are functional, as yeast cannot survive without *MYO2* (Johnston et al., 1991). Myo2p protein levels are also the same as wild-type except

for the 8-IQ variant which has ~75% of the wild-type level, and all variants allow slightly more frequent linear GFP–Sec4p movements than wild-type (Fig. 4, A, B, and C).

Strikingly, the maximum velocities recorded for each construct show a linear relationship with the number of IQ repeats (Fig. 4 E, Fig. 5 and Video 4, available at http://www.jcb.org/cgi/content/full/jcb.200110086/DC1), implying that this part of myosin-V acts as a simple rigid mechanical element in accordance with the lever-arm model. Note that GFP–Sec4p velocities are remarkably reproducible for particles following the same track (Fig. 4 E).

Most myosin-V/XIs have six IQ repeats of precisely conserved length. The observation that chicken myosin-V takes at least 40 steps for each encounter with actin, each step measuring 30–40 nm (Mehta et al., 1999; Rief et al., 2000; Sakamoto et al., 2000), might provide an explanation. The microfilament helix presents actin subunits in the same orientation only once every 36 nm, which might constrain a processive dimeric motor like myosin-V to make 36-nm steps in a hand-over-hand fashion if the lever arm model is correct (Rief et al., 2000; Mehta, 2001; Fig. 1 B). The myosin-V IQ repeat region is the correct length to allow a dimer to span the actin helix (Walker et al., 2000). In this light, it is remarkable that Myo2p variants with other than six IQ repeats are functional motors at all. However, the obstacle posed by the mismatch between the myosin-V's step size and the actin pseudorepeat might be overcome by side stepping to out-of-register filaments in an actin cable, or the presence of multiple Myo2p dimers per particle. Mismatches with the 36-nm actin pseudorepeat might account for the higher rate of nonmotile and pausing particles (Fig. 4 D) and greater scatter in transport velocities observed for mismatched myosin-Vs compared with the natural myosin-V (Fig. 5).

The availability of a live-cell myosin motor assay in an organism that allows easy transformation, gene replacement, and large-scale genetic screening opens up a new approach that will facilitate additional studies of how myosin produces force.

In summary, the effect of Myo2p IQ repeat number on GFP–Sec4p velocity unambiguously demonstrates that a myosin-V directs secretion by actively transporting membranes and shows that the IQ repeat region acts as a mechanical amplifier in vivo.

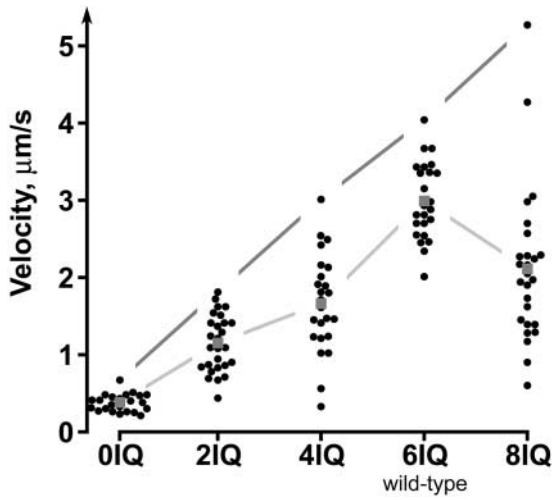

Figure 5. **Effect of lever arm length on velocity.** Scatter plot of GFP–Sec4p particle velocities (circles). Dark gray lines connect the highest velocity for each strain. Light gray lines connect the mean velocity (gray squares) for each strain. See Video 4, available at http://www.jcb.org/cgi/content/full/jcb.200110086/DC1.

Materials and methods

GFP–Sec4p

The yeast centromere plasmid pRC556 contains the *YOP1* 5′ untranslated region from nucleotide –445 to –1, fused directly to the complete yEGFP coding region (encoding *mut3*GFP) (Cormack et al., 1997), fused directly to the *SEC4* open reading frame (missing the initial ATG), plus the *SEC4* 3′ untranslated region. We constructed pRC556 by amplifying the *YOP1* promoter, yEGFP, and *SEC4* with overlapping oligonucleotide primers and subcloning the amplified product into the centromeric yeast vector pRS315 (Sikorski and Hieter, 1989). pRC556 completely suppresses the temperature-sensitive growth defect of *sec4–8* yeast at 37°C, indicating that the *mut3*GFP–Sec4p fusion protein is functional. In addition, like duplication of wild-type *SEC4* (Salminen and Novick, 1987), pRC556 completely suppresses the growth defect of a *sec2–41* mutant at 33°C and partially suppresses *sec2–41* at higher temperatures.

Yeast strains with varying numbers of IQ repeats in *MYO2*

We cloned *MYO2+* and *MYO2Δ6IQ* (called 0IQ here) (Stevens and Davis, 1998) into a pRS303-integrating vector as described (Schott et al., 1999) and altered the *MYO2* gene by amplifying the IQ repeat region with appropriate primers and splicing back into *MYO2* on the plasmid. The uniform 48 amino acid spacing of IQ repeat pairs allowed us to perform precise deletions and duplication. Numbering the myosin-V IQ repeats 1-2-3-4-5-6, the sequences of the new alleles are as follows (with primer sequences in parentheses): 2IQ, 1-6 (AATATTACCGTAAGCAGTATTTGCAAATAAAAAAAGACACTGTTGTTGTCCAAT); 4IQ, 1-2-3-6 (GTGCCAATGTGTTCAGCGTAAAAAAAGACACTGTTGTTGTCCAAT); and 8IQ, 1-2-3-4-3-4-5-6 (AAAGACAACTGAAACAAGAACATGAAGTTAACTGTGCAACTTTATTACAGGCC). Integration of these five plasmids into the haploid yeast strain CRY1 (Stevens and Davis, 1998) resulted in a series of five isogenic strains, differing only in the number of IQ repeats in *MYO2*, and containing the pRS303-integrating plasmid inserted between the *MYO2* and *SNC2* genes. All strains express *mut3*GFP–Sec4p from a *YOP1* promoter on the centromere plasmid pRC556 described above. We confirmed that only one version of *MYO2* is present in each of the five strains by electrophoresis of amplified *MYO2* DNA, and confirmed the new alleles to be error-free by sequencing the amplified genomic DNA.

Observation of live cells

We mounted yeast cells on agarose containing 4% glucose synthetic medium, and observed them at 22–24°C under a conventional fluorescence microscope with a 100× objective (NA 1.3) and a CCD detector, collecting 50-ms exposures at a rate of nine exposures per second. We recorded and viewed the digital images using the MetaMorph® software package (Universal Imaging Corporation). We measured velocities as displacement of particle images over time, excluding movements close to the bud neck where the particles tend to slow down. Velocities may be slight underestimates because we did not take into account movement perpendicular to the focal plane and pauses shorter than 0.5 s.

Temperature-sensitive strains

We introduced pRC556 (the *mut3*GFP–Sec4p expression plasmid) into ABY536 (*myo2–16*), ABY531 (*MYO2*), ABY988 (*tpm1–2 tpm2Δ*), and ABY987 (*TPM1 tpm2Δ*) (Pruyne et al., 1998; Schott et al., 1999), and used a thermostat-controlled objective heater to perform temperature shifts.

Measurement of relative Myo2p levels

To determine semiquantitative Myo2p levels in the IQ variant strains relative to wild-type, we grew the five yeast strains to an optical density of 0.4 units in minimal medium, chilled the cultures on ice, washed two optical density units of each strain in water, resuspended them in 150 μl chilled buffer (50 mM Tris-HCl, 5 mM Na-EDTA, and 5% SIGMA yeast protease inhibitor cocktail in DMSO), added 500-μl glass beads, agitated them for 5 min in a bead beater at 4°C to open >90% of the cells, added SDS-PAGE

sample buffer, boiled them for 3 min, centrifuged out the cell walls, and immediately loaded on a 6% polyacrylamide gel. We loaded two or three dilutions of each sample to determine the approximate relationship between the amount of sample and the amount of signal. We blotted the gel onto nitrocellulose and stained with Ponceau S to confirm equal loads for each strain. We then detected Myo2p using an affinity-purified antibody to the Myo2p COOH-terminal tail, a peroxidase-coupled secondary antibody, and the 3,3′-diaminobenzidine reaction to detect the peroxidase. We performed the experiment, from sample preparation to immunodetection, twice to confirm results.

Online supplemental material

Video 1 shows the transit of a GFP–Sec4p particle across a mother cell to the bud neck. Video 2 shows several GFP–Sec4p particles taking the same path across a mother cell and into the bud. These particles also follow defined paths across the bud to the bud cortex, and at least two can be seen to reach the bud tip. Video 3 shows Brownian motion of GFP–Sec4p particles in a *tpm1–2 tpm2Δ* and two *myo2–16* cells shifted to the restrictive temperature. Video 4 shows a comparison of GFP–Sec4p movement in wild-type and 0IQ cells. Videos are available at http://www.jcb.org/cgi/content/full/jcb.200110086/DC1.

We thank Trisha Davis (University of Washington, Seattle, WA) for the 0IQ allele, Janet Ingraffea (Cornell University, Ithaca, NY) for anti-Myo2p tail antibody, and Tim Huffaker for the use of his microscope.

This study was funded by the National Institutes of Health (GM39066 to A. Bretscher).

Submitted: 16 October 2001
Revised: 28 November 2001
Accepted: 28 November 2001

References

Ayscough, K.R., J. Stryker, N. Pokala, M. Sanders, P. Crews, and D. Drubin. 1997. High rates of actin filament turnover in budding yeast and roles for actin in establishment and maintenance of cell polarity revealed using the actin inhibitor latrunculin-A. *J. Cell Biol.* 137:399–416.

Cheney, R.E., M.K. O'Shea, J.E. Heuser, M.V. Coelho, J.S. Wolenski, E.M. Espreafico, P. Forscher, R.E. Larson, and M.S. Mooseker. 1993. Brain myosin-V is a two-headed unconventional myosin with motor activity. *Cell.* 75: 13–23.

Cormack, B.P., G. Bertram, M. Egerton, N.A.R. Gow, S. Falkow, and A.J.P. Brown. 1997. Yeast-enhanced green fluorescent protein (yEGFP): a reporter of gene expression in *Candida albicans*. *Microbiology.* 143:303–311.

Corti, B. 1774. Saggio d'osservazioni sulla circolazione del fluido scoperto in una pianta acquajuola appellata cara. *In* Osservazione de fluido in una pianta acquajuola. Appresso Giuseppe Rocchi, Lucca, Italy. 125–200.

Geeves, M.A., and K.C. Holmes. 1999. Structural mechanism of muscle contraction. *Annu. Rev. Biochem.* 68:687–728.

Govindan, B., R. Bowser, and P. Novick. 1995. The role of Myo2, a yeast class V myosin, in vesicular transport. *J. Cell Biol.* 128:1055–1068.

Houdusse, A., and H.L. Sweeney. 2001. Myosin motors: missing structures and hidden springs. *Curr. Opin. Struct. Biol.* 11:182–194.

Johnston, G.C., J.A. Prendergast, and R.A. Singer. 1991. The *Saccharomyces cerevisiae MYO2* gene encodes an essential myosin for vectorial transport of vesicles. *J. Cell Biol.* 113:539–551.

Kashiyama, T., N. Kimura, T. Mimura, and K. Yamamoto. 2000. Cloning and characterization of a myosin from characean alga, the fastest motor protein in the world. *J. Biochem.* 127:1065–1070.

Mehta, A. 2001. Myosin learns to walk. *J. Cell Sci.* 114:1981–1998.

Mehta, A.D., R.S. Rock, M. Rief, J.A. Spudich, M.S. Mooseker, and R.E. Cheney. 1999. Myosin-V is a processive actin-based motor. *Nature.* 400:590–593.

Mulholland, J., A. Wesp, H. Riezman, and D. Botstein. 1997. Yeast actin cytoskeleton mutants accumulate a new class of Golgi-derived secretory vesicle. *Mol. Biol. Cell.* 8:1481–1499.

Pruyne, D.W., D.H. Schott, and A. Bretscher. 1998. Tropomyosin-containing actin cables direct the Myo2p-dependent polarized delivery of secretory vesicles in budding yeast. *J. Cell Biol.* 143:1931–1945.

Reck-Peterson, S.L., D.W. Provance, Jr., M.S. Mooseker, and J.A. Mercer. 2000. Class V myosins. *Biochim. Biophys. Acta.* 1496:36–51.

Rief, M., R.S. Rock, A.D. Mehta, M.S. Mooseker, R.E. Cheney, and J.A. Spudich. 2000. Myosin-V stepping kinetics: a molecular model for processivity. *Proc. Natl. Acad. Sci. USA.* 97:9482–9486.

Ruff, C., M. Furch, B. Brenner, D.J. Manstein, and E. Meyhofer. 2001. Single-molecule tracking of myosins with genetically engineered amplifier domains. *Nat. Struct. Biol.* 8:226–229.

Sakamoto, T., I. Amitani, E. Yokota, and T. Ando. 2000. Direct observation of processive movement by individual myosin V molecules. *Biochem. Biophys. Res. Commun.* 272:586–590.

Salminen, A., and P.J. Novick. 1987. A ras-like protein is required for a post-Golgi event in yeast secretion. *Cell.* 49:527–538.

Schott, D., J. Ho, D. Pruyne, and A. Bretscher. 1999. The COOH-terminal domain of Myo2p, a yeast myosin V, has a direct role in secretory vesicle targeting. *J. Cell Biol.* 147:791–808.

Sikorski, R.S., and P. Hieter. 1989. A system of shuttle vectors and yeast host strains designed for efficient manipulation of DNA in *Saccharomyces cerevisiae*. *Genetics.* 122:19–27.

Stevens, R.C., and T.N. Davis. 1998. Mlc1p is a light chain for the unconventional myosin Myo2p in *Saccharomyces cerevisiae*. *J. Cell Biol.* 142:711–722.

Trybus, K.M., E. Krementsova, and Y. Freyzon. 1999. Kinetic characterization of a monomeric unconventional myosin V construct. *J. Biol. Chem.* 274:27448–27456.

Uyeda, T.Q., P.D. Abramson, and J.A. Spudich. 1996. The neck region of the myosin motor domain acts as a lever arm to generate movement. *Proc. Natl. Acad. Sci. USA.* 93:4459–4464.

Walch-Solimena, C., R.N. Collins, and P.J. Novick. 1997. Sec2p mediates nucleotide exchange on Sec4p and is involved in polarized delivery of post-Golgi vesicles. *J. Cell Biol.* 137:1495–1509.

Walker, M.L., S.A. Burgess, J.R. Sellers, F. Wang, J.A. Hammer, III, J. Trinick, and P.J. Knight. 2000. Two-headed binding of a processive myosin to F-actin. *Nature.* 405:804–807.

Wu, X., B. Bowers, K. Rao, Q. Wei, and J.A. Hammer, III. 1999. Visualization of melanosome dynamics within wild-type and dilute melanocytes suggests a paradigm for myosin V function in vivo. *J. Cell Biol.* 143:1899–1918.

Yanagida, T., and A.H. Iwane. 2000. A large step for myosin. *Proc. Natl. Acad. Sci. USA.* 97:9357–9359.

Yanagida, T., S. Esaki, A.H. Iwane, Y. Inoue, A. Ishijima, K. Kitamura, H. Tanaka, and M. Tokunaga. 2000a. Single-motor mechanics and models of the myosin motor. *Philos. Trans. R. Soc. Lond. B Biol. Sci.* 355:441–447.

Yanagida, T., K. Kitamura, H. Tanaka, A. Hikikoshi-Iwane, and S. Esaki. 2000b. Single molecule analysis of the actomyosin motor. *Curr. Opin. Cell Biol.* 12: 20–25.